Journal of GeoEngineering, Vol. 17, No. 4, pp. 175-187, December 2022
http://dx.doi.org/10.6310/jog.202212_17(4).1

DISTRIBUTION CHARACTERISTICS OF SURFACE DISPLACEMENT DUE TO LATERAL SPREADING OF LIQUEFIED GROUND

Yung-Yen Ko [1*], Tri Kurnia Rahayu.J [2]

ABSTRACT

This study aimed to characterize the distribution of surface displacement caused by lateral spreading of liquefied ground based on field measurement data. Cases of lateral spreading during the 1995 Hanshin Awaji, Japan earthquake, the 1999 Chi-Chi, Taiwan earthquake, and the 2010 Darfield, New Zealand earthquake were selected for investigation. The displacement distribution was regressed by existing logarithmic decay and exponential decay models and two newly proposed models based on normal and log-normal complementary cumulative distribution functions. The R-squared value was adopted to evaluate the performance of the models for regression analysis. The results show that the logarithmic decay model satisfactorily approximated the surface displacement distribution in most of the cases, and the exponential decay model was applicable for cases that attenuates with distance most significantly near the waterfront. By contrast, the normal and log-normal complementary cumulative distribution functions gave good approximation for the displacement distribution with a double-curvature feature related to the "block-mode" failure. The ratio of the length of laterally spreading area to the waterfront displacement was also examined, and its range in some cases are roughly conformable to existing study whereas is obviously larger in the 2010 Darfield earthquake case.

Key words: Soil liquefaction, lateral spreading, surface displacement distribution, regression analysis.

1. INTRODUCTION

Lateral spreading of the ground is recognized as one of the most devastating types of ground failure caused by liquefaction. It is characterized by horizontal displacement of non-liquefied surface layers (also referred to as crust) as a consequence of liquefaction of an underlying granular deposit, usually accompanied with surface cracks or even with surface layers broken into blocks (Youd 1995), as shown in Fig. 1. Lateral spreading can be generally divided into two types (Youd 2008), one is towards a free face (*e.g.,* riverbank or seashore), which gives an unrestricted boundary, and the other is down a gentle slope, which is less than 6% or flow failure may occur (Youd 1995). Lateral spreading may cause open fissures on the ground surface and buckling of soil or pavement at zones of extension and compression it creates, respectively; it may also damage piles embedded in the laterally moving soil which imposes lateral force on them; for the waterfront area, it can damage waterfront structures such as levees, revetments and quay walls (Hamada 1992; Lin *et al.* 2006; Youd 2008).

The 1964 M_w 7.6 Niigata earthquake in Japan, along with the M_w 9.2 Alaska earthquake in United States in the same year, awaked the geotechnical engineers to the potential of soil liquefaction to cause damage during earthquakes (Youd 2014). During Niigata earthquake, a huge amount of ground distortion induced by liquefaction in terms of settlement and lateral spreading was reported, and one representative case was the Showa bridge, which had been successfully constructed 3 months before the earthquake yet was damaged due to the lateral spreading towards the waterfront. In 1995, the M_w 6.9 Hanshin Awaji, Japan earthquake (also known as Kobe earthquake) caused severe liquefaction in the reclaimed island, and the laterally spreading ground dislocated many quay walls in the port area and ruined their serviceability. The M_w 7.6 Chi-Chi earthquake struck Taiwan in 1999 and resulted in extensive loss of human lives and properties; although liquefaction-induced lateral spreading was not responsible for the majority of the loss, it was observed at several different riverside locations. The three relatively major events of the 2010-2011 Canterbury, New Zealand earthquake sequence, including the 2010 M_w 7.1 Darfield earthquake (mainshock), as well as the 2011 February M_w 6.2 and 2011 June M_w 6.0 Christchurch earthquakes (aftershocks), caused not only severe structural damage in downtown Christchurch but also widespread repeated liquefaction in the residential suburbs (Cubrinovski *et al.* 2012). The lateral spreading near riverbank and lakeside brought substantial damages to residential

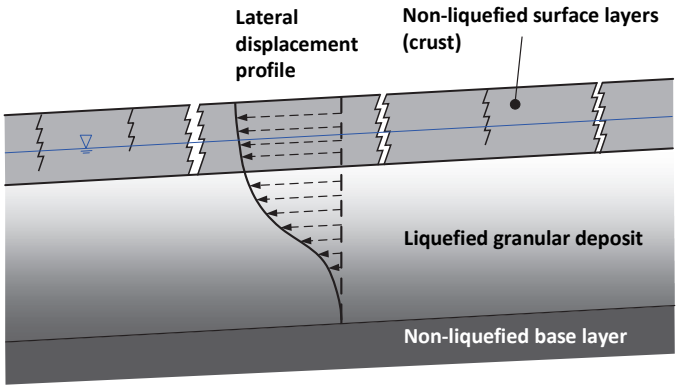

Fig. 1 General features of liquefaction-induced lateral spreading (after Rauch 1997 and Youd 2018)

Manuscript received May 31, 2022; revised June 25, 2022; accepted August 1, 2022.
[1*] Associate Professor (corresponding author), Department of Civil Engineering, National Cheng Kung University, Tainan, Taiwan (e-mail: yyko@ncku.edu.tw).
[2] Lecturer, Civil Engineering Department, State Polytechnic of Sriwijaya, Palembang, Indonesia.

buildings and lifelines, especially in the 2011 February aftershock. All these cases revealed the hazard of the liquefaction-induced lateral spreading, especially the towards-free-face type.

For the mitigation of lateral spreading of liquefied ground, it is essential to capture the distribution characteristics of the ground displacement so that its magnitude and affected range can be estimated with satisfactory accuracy. Although some models for surface displacement distribution of laterally spreading ground have been proposed and widely used, the actual situation may differ considerably from case to case so that a universally applicable model seems not available. Hence, this study examined several models for surface displacement distribution to assess their performance of approximation for different cases of towards-free-face type lateral spreading during historical major earthquakes, including two well-known ones, the logarithmic decay (Bartlett and Youd 1995) and exponential decay (Tokimatsu and Asaka 1998), as well as two newly proposed ones based on normal and log-normal complementary cumulative distribution functions. In addition, the relationship of affected range of lateral spreading versus the waterfront displacement for each investigated case was also discussed. The results can serve as the reference for disaster reduction in geotechnical earthquake engineering aspects.

2. MODELS FOR SURFACE DISPLACEMENT DISTRIBUTION OF LATERAL SPREADING GROUND

2.1 Logarithmic Decay Model (Bartlett and Youd 1995)

Bartlett and Youd (1995) demonstrated that the ground surface displacement along Shinano River induced by lateral spreading during the 1964 Niigata earthquake showed roughly logarithmic decay with the distance to the free face (*i.e.,* the waterfront), as shown in Fig. 2, with the regression equation as Eq. (1):

$$D(x) = 11.6 - 4.38 \log x \tag{1}$$

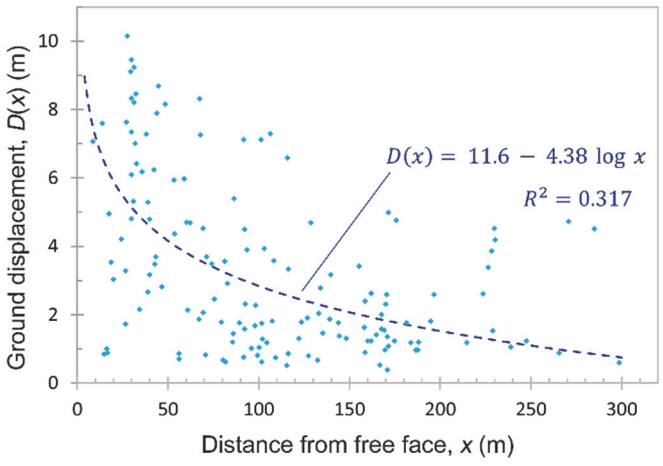

Fig. 2 Ground surface displacement along Shinano River during the 1964 Niigata earthquake (after Bartlett and Youd 1995)

where $D(x)$ is the horizontal surface displacement at ground at the observation point, and x is the distance from the observation point to the waterfront.

Although Eq. (1) represents the best fit curve, it has a low R-squared value (R^2) of 0.317. This is possibly because the ground displacement was measured at scattered points within the range of laterally moving ground instead of along specific lines to obtain displacement distribution profiles, and then all the data were mixed for regression analysis, leading to a not quite satisfactory result.

With additional geographical, geological, and soil parameters, the multiple linear regression (MLR) procedure was further proposed for prediction of lateral spread displacement (Bartlett and Youd 1995; Youd *et al.* 2002).

In this study, the logarithmic decay model for regression analysis is transformed into Eq. (2), in which the surface displacement and the waterfront distance are normalized for more generalized application.

$$\frac{D(x)}{D_0} = a \ln\left(\frac{x}{L}\right) + b \tag{2}$$

where D_0 denotes the surface displacement at waterfront; L denotes the length of laterally spreading area (from where the displacement is negligible to the waterfront).

Note that the waterfront displacement will be excluded in the regression analysis using logarithmic decay model because $\ln(0)$ is not defined mathematically. In addition, Eq. (2) cannot be applied to the surface displacement data in Fig. 2 because these data were not measured along specific lines so that the length of laterally spreading area cannot be defined.

2.2 Exponential Decay (Tokimatsu and Asaka 1998)

According to the ground displacement investigation of lateral spreading near waterfront areas during 1995 Hanshin Awaji earthquake (Shamoto and Hotta 1996; Ishihara *et al.* 1997; Yasuda *et al.* 1997), Tokimatsu and Asaka (1998) proposed the relationship of horizontal surface displacement versus the distance to the waterfront as Eq. (3):

$$\frac{D(x)}{D_0} = \left(\frac{1}{2}\right)^{\frac{5x}{L}} \tag{3}$$

Equation (3) suggests that the horizontal surface displacement decreases to half of that at waterfront at $x = L/5$ and to less than 20% at $x = L/2$.

Tokimatsu and Asaka (1998) also suggested that L = (25-100)D_0 based on Shamoto and Hotta (1996), Tokimatsu *et al.* (1997) and Yasuda *et al.* (1997), and $L = 50D_0$ can be regarded as representative. In this study, in addition to $D(x)$ versus x relationship, the ratio of L to D_0 will also be examined in each investigated case.

The exponential decay model for regression analysis in this study is in the following form:

$$\frac{D(x)}{D_0} = \left(\frac{1}{2}\right)^{\frac{cx}{L}} \tag{4}$$

The one-parameter feature (only an undetermined multiplier in the exponent but not in the base) of Eq. (3) assures that $D(0)$ is always equal to D_0.

2.3 Normal and Log-Normal Complementary Cumulative Distribution Functions

In both logarithmic decay and exponential decay models, the decay of surface displacement with the distance to the waterfront is significant in the beginning and gets smaller as the distance increases. However, in some lateral spreading cases, such as those in South Kaiapoi during the 2010 M_w 7.1 Darfield earthquake (to be presented in Section 3.3), the decay rate of surface displacement was not highest near the waterfront but at a certain distance away. Thus, $D(x)$ curve might exhibit double curvature (namely, with an "S" shape), and consequently neither logarithmic decay nor exponential decay can give a satisfactory approximation of it.

For curves with a double-curvature feature, the normal cumulative distribution function (CDF), $F(x)$, can be used for approximation:

$$F(x) = \int_{-\infty}^{x} f(\xi)\, d\xi = \Phi\left(\frac{x-\mu}{\sigma}\right) \tag{5}$$

where $f(x)$ is the probability density function (PDF) of normal distribution of a random variable x with a mean (or median) μ and a standard deviation σ, as given in Eq. (6):

$$f(x) = \frac{1}{\sigma\sqrt{2\pi}} e^{-\frac{1}{2}\left(\frac{x-\mu}{\sigma}\right)^2} \quad ; \quad -\infty < x < \infty \tag{6}$$

$f(x)$ in Eq. (6) has a symmetric virtue and a bell-shaped feature and is widely used to represent the probability distribution of many natural processes. Besides, Φ in Eq. (5) denotes the CDF of the standard normal distribution.

Considering the nature that the horizontal surface displacement of lateral spreading ground is largest at the waterfront and decreases with the distance to the waterfront, the complement of the normal CDF, or the normal complementary cumulative distribution function (CCDF, also known as the tail distribution function) can be used to approximate $D(x)$:

$$\frac{D(x)}{D_0} = 1 - \Phi\left(\frac{\hat{x}-\hat{\mu}}{\hat{\sigma}}\right) \tag{7}$$

where $\hat{x}$ denotes x/L; $\hat{\mu}$ and $\hat{\sigma}$ are the mean and the standard deviation of $\hat{x}$, respectively.

With a similar idea, the log-normal CDF, that is, the CDF of log-normal PDF (the logarithm of its random variable is normally distributed), can also be used to approximate an S-shaped curve. For example, in the earthquake loss estimation methodology HAZUS 99 (FEMA 1999), the seismic fragility curves were parameterized by the lognormal CDF. Therefore, $D(x)$ can also be approximated by log-normal CCDF:

$$\frac{D(x)}{D_0} = 1 - \Phi\left(\frac{\ln\hat{x} - \hat{\mu}^*}{\hat{\sigma}^*}\right) \tag{8}$$

where $\hat{\mu}^* = \exp(\hat{\mu})$ and $\hat{\sigma}^* = \exp(\hat{\sigma})$.

Similar to logarithmic decay model, Eq. (8) is not applicable for $\hat{x} = 0$. However, because log-normal CCDF approaches 1 as x approaches 0, $\hat{x} = 10^{-6}$ was used instead of $\hat{x} = 0$, which hardly influenced the result of regression.

3. FIELD DATA OF LATERAL SPREADING DISPLACEMENT

Selected field data of ground surface displacement caused by towards-free-face lateral spreading during three historical major earthquakes are presented in this section. Noted that only those given in the form of displacement profile (namely, measured along a specific line) are included so that the distribution of surface displacement with distance can be reasonably revealed, and the data are presented in terms of $D(x)/D_0$ versus x/L.

3.1 1995 Hanshin Awaji Earthquake – Port of Kobe

Ishihara *et al.* (1997) proposed a "method of ground surveying" for post-earthquake ground deformations and applied this idea to made field measurement of the lateral spreading induced by the extensive liquefaction over the near-waterfront areas of reclaimed lands in Kobe during the 1995 Hanshin Awaji, Japan earthquake. This method is achieved by measuring the width of crack opening and the distance between the cracks sequentially along a line perpendicular to the waterfront alignment which is representative of the ground rupture in the area to be investigated, and then summing up the widths of the cracks from the datum point to obtain the displacement distribution as function of distance to the waterfront. Several surface displacement profiles at three man-made islands in the Port of Kobe, Port Island (P), Rokko Island (R), and Fukaehama Island (F), with the survey lines as shown in Fig. 3, are adopted for investigation in this study.

Based on the boring data presented in Ishihara *et al.* (1997), the ground of the three islands is mainly composed of 15-23 m thick reclaimed sand deposit overlying silty clay. The blow counts of standard penetration test (SPT-N values) of the reclaimed deposit are generally around or below 10, and the groundwater table was around a depth of 1-2 m during the boring. Therefore, nearly all submerged reclaimed deposit can be considered liquefiable.

During the 1995 Hanshin Awaji earthquake, the horizontal peak ground acceleration (PGA) at Port Island reached 340.6 gal (in NS direction) and the duration of shaking was more than 30

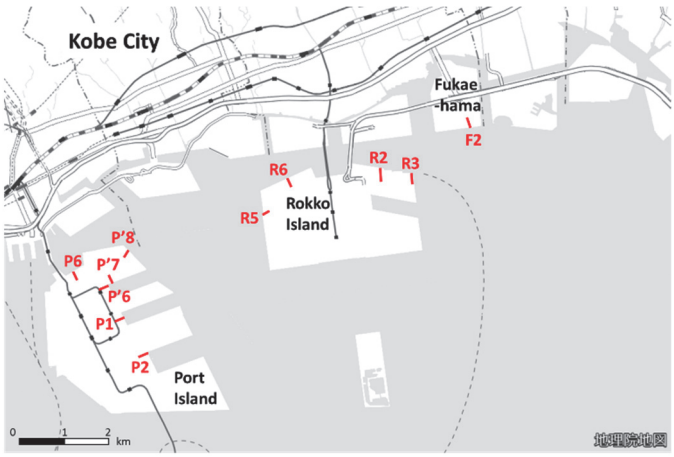

Fig. 3 Survey lines for surface displacement caused by lateral spreading in the Port of Kobe during 1995 Hanshin Awaji earthquake (after Ishihara *et al.* 1997; base map provided by Geospatial Information Authority of Japan)

seconds (Iwasaki and Tai 1996). Note that de-amplification of the higher-frequency components was observed by the vertical seismometer array because of a decrease in the soil moduli due to soil liquefaction (Iwasaki and Tai 1996), making the predominant frequency of surface motion around 0.5-0.7 Hz (Madabhushi 1995).

The data are divided into two groups, with north or south facing quay walls and with east or west facing quay walls, as depicted in Figs. 4(a) and 4(b), respectively, because the difference between the accelerations in north-south and east-west directions may somewhat affect the lateral displacement. The displacement profiles in both groups generally showed most significant decay near the waterfront. The reason could be that 90% of the quay walls in the Port of Kobe are of a caisson type, and most of the caisson walls were displaced toward sea partially because of the seismic inertia force (Iai *et al.* 1997). Consequently, the ground displacement by the waterfront was apparently larger than at the backland.

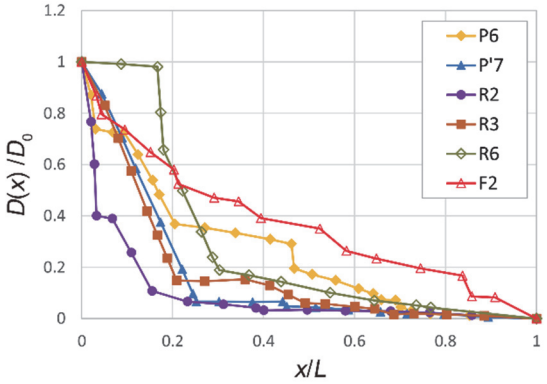

(a)

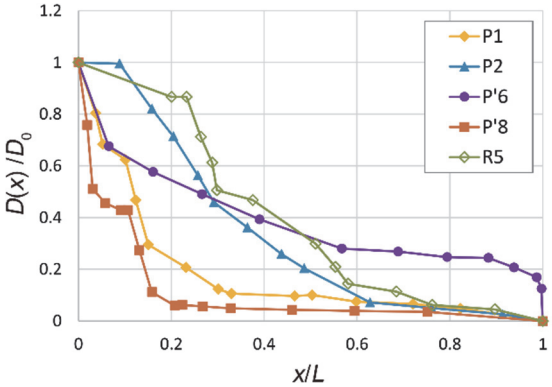

(b)

Fig. 4 Surface displacement profiles caused by lateral spreading in the Port of Kobe during 1995 Hanshin Awaji earthquake: (a) with north or south facing quay walls; (b) with east or west facing quay walls (after Ishihara *et al.* 1997)

3.2 1999 Chi-Chi Earthquake – Central Taiwan

Detailed field survey of the location and opening width of ground cracks caused by lateral spreading was made at two sites in central Taiwan that suffered lateral spreading of riverbank during 1999 Chi-Chi, Taiwan earthquake, including survey line Pr1 by Maoluo River near the Nangang Bridge in Nantou (Hwang *et al.* 2000) and survey lines Pr2-Pr6 by the branches of Gan River in WuFeng, Taichung (Lin 2002), as shown in Fig. 5.

The soil profiles of Pr1 and Pr6 are both a silty sand layer (5-10 m thick; SPT-N around 5-20) overlying much stiffer gravel and stiff clay, respectively (Hwang *et al.* 2000; Lin 2002). Hence, the lateral spreading should be due to the liquefaction of upper silty sand layer. On the other hand, the ground at Pr2-Pr5 is composed of the upper silty sand layer and the underlying interlayered silt, silty sand and silty clay; however, by examining sand boil ejecta and the boring logs, Lin (2002) concluded that liquefaction at Pr2-Pr5 occurred from the groundwater table (at a depth of around 3-4 m) to a depth of around 4-9 m. Therefore, all the data in this case were associated with lateral spreading to a relatively shallower depth than the Port of Kobe case.

At the nearest seismic station to aforementioned sites, TCU065, the 1999 Chi-Chi earthquake caused a PGA up to 774 gal (in EW direction, data provided by http://scweb.cwb.gov.tw) and a shaking duration as long as 1 minute. Note that amplification of seismic waves at around 1-2 Hz with characteristic spiky waveforms in the acceleration time history was observed, which could be related to soil nonlinearity and liquefaction (Pavlenko and Wen 2008).

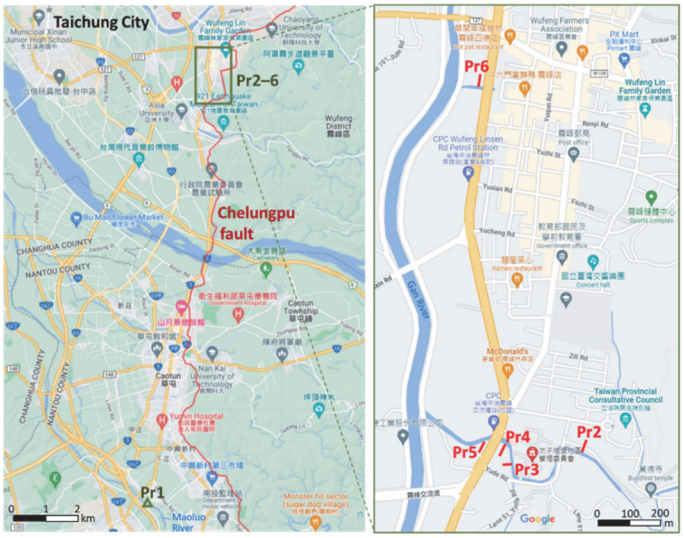

Fig. 5 Survey lines for ground cracks caused by lateral spreading in central Taiwan during 1999 Chi-Chi earthquake (after Hwang *et al.* 2000 and Lin 2002; base map provided by Google Map)

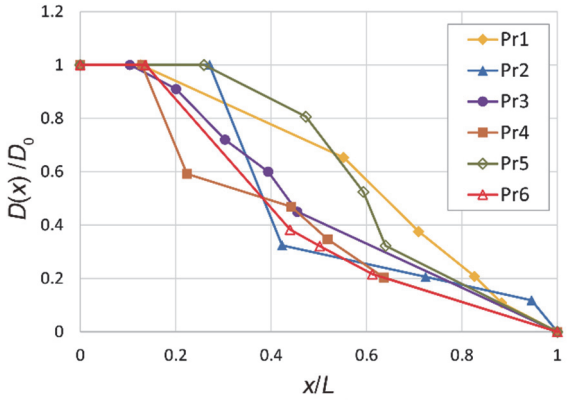

Fig. 6 Surface displacement profiles caused by lateral spreading in central Taiwan during 1999 Chi-Chi earthquake (based on Hwang *et al.* 2000 and Lin 2002)

Based on these survey data, the surface displacement profiles were calculated using the method of Ishihara *et al.* (1997), as shown in Fig. 6. The decay of displacement with distance in all investigated profiles was not as significant as that in the Port of Kobe in the previous section. Note that all the data in this case were from lateral spreading of riverbanks. Despite some of them with revetments, less inertial effect was involved because the revetment is a retaining structure not as massive as the caisson quay wall, and this could be the reason of aforementioned difference.

3.3 2010 Darfield Earthquake – Kaiapoi

During the 2010 Darfield, New Zealand earthquake, the waterfront area in Kaiapoi (north to Christchurch) experienced massive lateral spreading, and detailed survey of the induced ground displacement was made over this area following the procedure proposed by Ishihara *et al.* (1997) afterwards (Cubrinovski *et al.* 2012; Robinson 2016). These data were divided into two groups, North Kaiapoi and South Kaiapoi; the former was obtained along the Kaiapoi River, and the latter was along Courtenay Stream and Courtenay Lake, as shown in Fig. 7.

According to data of cone penetration test (CPT) to a depth of around 10 m, the soil in North Kaiapoi is identified to be mainly medium dense to dense coarse sand in the northwest (except that above the depth of 2.5 m is soft) and grading to loose silty fine sand downstream, whereas the soil in South Kaiapoi is generally very soft and loose (Robinson 2016). In both North and South Kaiapoi, the groundwater table was generally around a depth of 1-2 m as CPT was conducting. Therefore, at least the near surface layer shows certain liquefaction potential in Kaiapoi area.

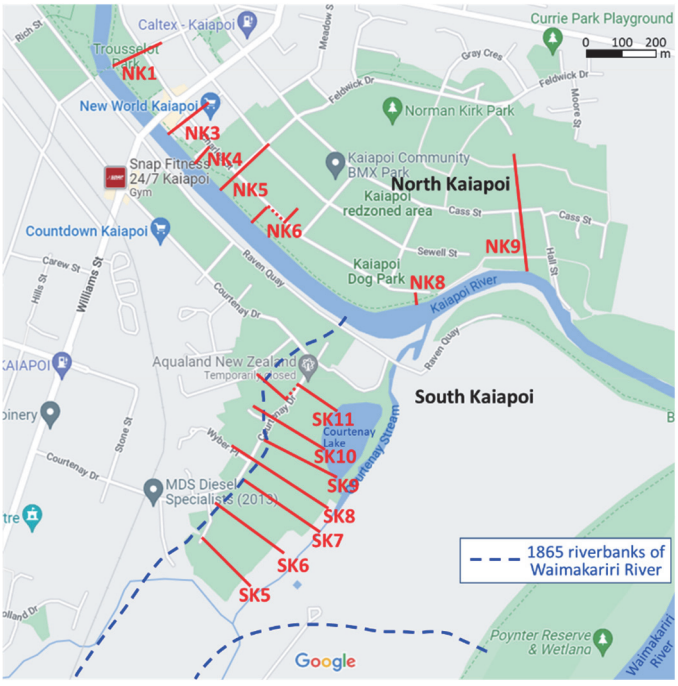

Fig. 7 Survey lines for surface displacement caused by lateral spreading in Kaiapoi during 2010-2011 Canterbury earthquake sequence (after Robinson 2016 and Wotherspoon *et al.* 2012; base map provided by Google Map)

A PGA of 408 gal was observed at the seismic station KPOC in Kaiapoi during the 2010 Darfield earthquake, and the shaking continued for more than 1 minute because of significant surface wave with a peak ground velocity of 20 cm/s and a period of 8 seconds. This extremely long period of surface wave with a source-to-site distance of 28 km could be due to a depth to basement up to 2 km (Bradley 2012).

The surface displacement profiles included for investigation are depicted in Fig. 8. Figure 8(a) shows that most of the surface displacement profiles in North Kaiapoi (except profile NK1) were similar to those in the Port of Kobe (refer to Section 3.1), as indicated by Cubrinovski *et al.* (2012); that is, more significant decay near the waterfront. By contrast, as shown in Fig. 8(b), the liquefied ground in South Kaiapoi exhibited the "block-mode" failure, which means that the ground from the waterfront to a certain distance (approximately 150 m) inland moved as a block with ground fissures opened up around this distance (Cubrinovski and Robinson 2016). This could be attributed to the paleochannel of Waimakariri River located beneath these survey lines (Cubrinovski *et al.* 2012; Wotherspoon *et al.* 2012), of which the riverbanks in 1865 are marked in Fig. 7. The block-mode failure made the displacement distribution curves generally exhibited a double-curvature feature.

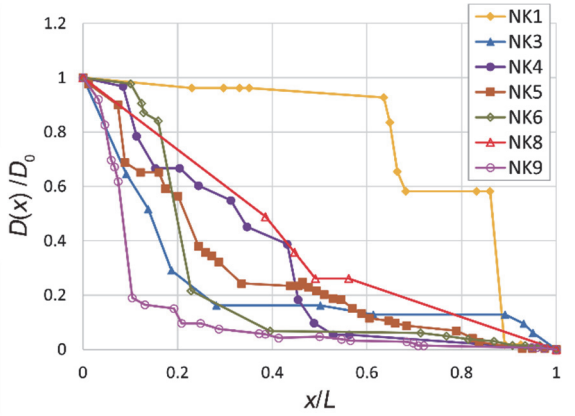

(a)

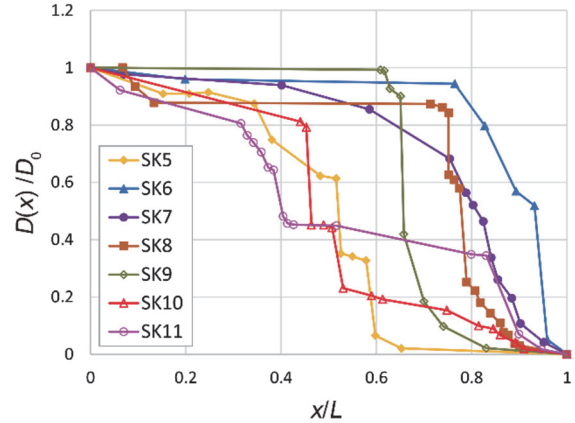

(b)

Fig. 8 Surface displacement profiles caused by lateral spreading in Kaiapoi during 2010 Darfield earthquake: (a) North Kaiapoi; (b) South Kaiapoi (after Robinson 2016)

4. REGRESSION ANALYSIS OF SURFACE DISPLACEMENT DISTRIBUTION

The surface displacement profiles examined in Section 3 were based on reliable field measurement, and therefore the models introduced in Section 2 were further used to perform regression analysis of these data so that the distribution characteristics of surface displacement of laterally spreading ground in different cases can be more clearly revealed. The results are presented as follows, and the performance of adopted models was assessed by R^2.

4.1 1995 Hanshin Awaji Earthquake – Port of Kobe

Because in this case the surface displacement generally decayed most significantly near the waterfront, only the logarithmic decay and exponential decay models (Eqs. (2) and (3)) were adopted for regression analysis. Firstly, taking profile P6 (with a north facing quay wall) for example, Fig. 9 shows that both decay models gave high values of R^2 which were close to 1. The estimated parameters of both models of all the profiles with north or south facing quay walls are summarized in Table 1(a), and a graphical comparison of R^2 is given in Fig. 11(a), which shows that a

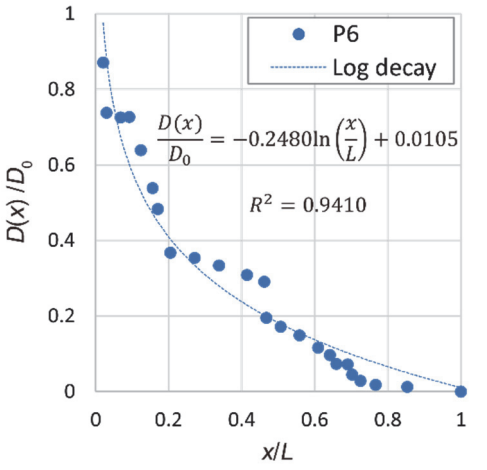

(a)

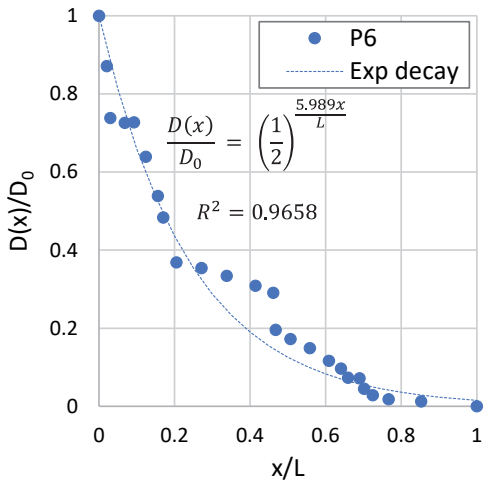

(b)

Fig. 9 Surface displacement regression of profile P6 in the Port of Kobe during 1995 Hanshin Awaji earthquake: (a) logarithmic decay; (b) exponential decay

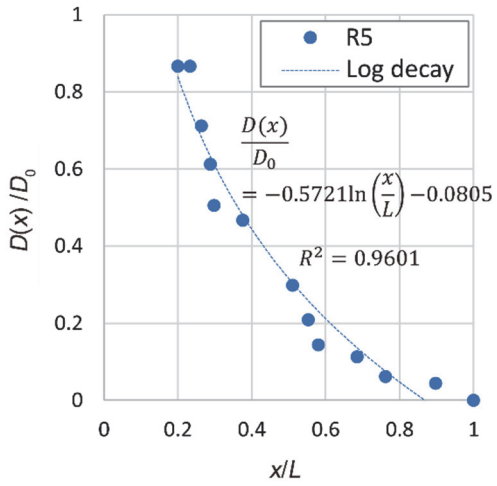

(a)

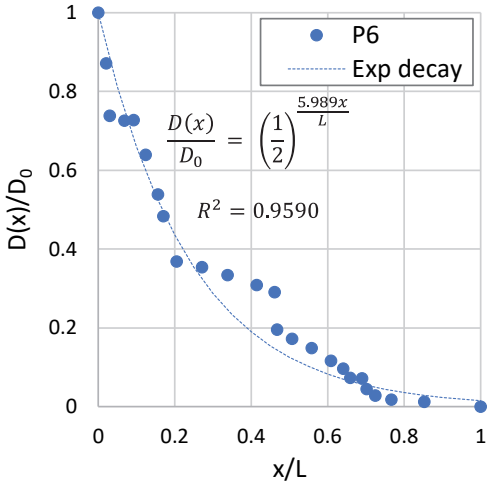

(b)

Fig. 10 Surface displacement regression of profile R5 in the Port of Kobe during 1995 Hanshin Awaji earthquake: (a) logarithmic decay; (b) exponential decay

Table 1 Estimated model parameters of surface displacement regression in the Port of Kobe during 1995 Hanshin Awaji earthquake: (a) with North or South facing quay walls; (b) with East or West facing quay walls

(a)

Survey line	Logarithmic decay			Exponential decay	
	a	*b*	R^2	*c*	R^2
P6	– 0.2480	0.0105	0.9410	5.989	0.9658
P'7	– 0.2866	– 0.1327	0.8378	8.566	0.9488
R2	– 0.1727	– 0.0835	0.8786	8.793	0.6525
R3	– 0.2709	– 0.0971	0.8971	7.782	0.9590
R6	– 0.4620	– 0.1543	0.8391	5.935	0.7746
F2	– 0.2421	0.1249	0.9400	3.519	0.9690

(b)

Survey line	Logarithmic decay			Exponential decay	
	a	*b*	R^2	*c*	R^2
P1	– 0.2489	– 0.0702	0.9224	6.399	0.9061
P2	– 0.4493	– 0.0662	0.9778	5.278	0.8390
P'6	– 0.2113	0.162	0.8990	2.706	0.8543
P'8	– 0.1915	– 0.1103	0.8553	9.445	0.7391
R5	– 0.5721	– 0.0805	0.9601	4.363	0.7457

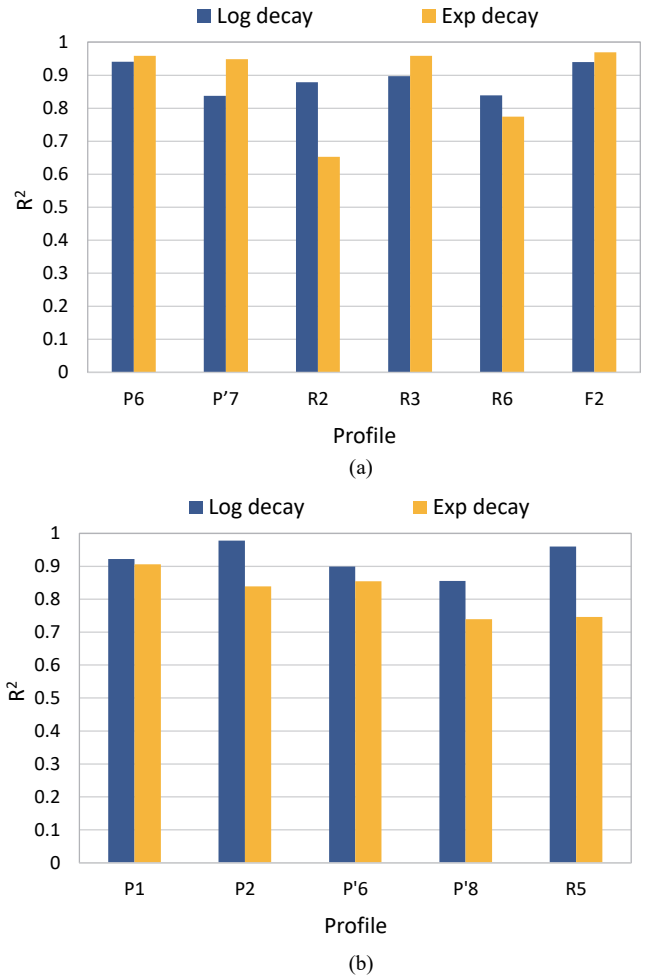

Fig. 11 Comparison of R^2 of surface displacement regression in the Port of Kobe during 1995 Hanshin Awaji earthquake: (a) with north or south facing quay walls; (b) with east or west facing quay walls

majority of the profiles had R^2 higher than 0.8. Furthermore, the exponential decay had R^2 around or above 0.95 in four out of six profiles, which may explain why Tokimatsu and Asaka (1998) chose it on the basis of the data from the Port of Kobe; on the other hand, R^2 of logarithmic decay showed more consistent tendency, all greater than 0.8, revealing its comparable performance to the exponential decay.

Another profile with a west facing quay wall, R5, can be regressed by the logarithmic decay with a high R^2 above 0.95, yet that of exponential decay regression is somewhat lower (about 0.75), as shown in Fig. 10. The estimated parameters of profiles with east or west facing quay walls are summarized in Table 1(b), and the R^2 comparison depicted in Fig. 11(b) indicates that logarithmic decay gave more accurate regression than exponential decay for these profiles.

To sum up, both logarithmic decay and exponential decay models can satisfactorily approximate the surface displacement of laterally spreading ground in the Port of Kobe during 1995 Hanshin Awaji earthquake, which features most significant attenuation near the waterfront; the logarithmic decay showed generally better performance, yet this could be associated with the exclusion of waterfront displacement in logarithmic decay regression.

4.2 1999 Chi-Chi Earthquake – Central Taiwan

In this case, the decay of surface displacement near the waterfront was not as significant as in the previous section, so all the four models introduced in Section 2 were used for regression analysis. Taking profile Pr5 for instance, Fig. 12 depicts that normal CCDF had a R^2 up to 0.97, and both logarithmic decay and log-normal gave good approximation with R^2 around 0.9, whereas R^2 exponential decay was somewhat lower. Table 2 summarizes the estimated parameters and Fig. 13 compares all the values of R^2 of all the examined profiles, which show that the logarithmic decay performs better in this case because of its consistently high R^2 compare with the other models. However, note that normal and log-normal CCDF gave good approximation (R^2 up to 0.9) for some of the profiles that exhibited a certain double-curvature feature (such as Pr5).

4.3 2010 Darfield Earthquake – Kaiapoi

Section 3.3 showed that most of the profiles in North Kaiapoi had displacement distribution similar to those in the Port of Kobe, and one of them, NK5, is adopted herein to demonstrate the regression, as depicted in Fig. 14. Not surprisingly the logarithmic decay and exponential decay models gave good approximation, whereas the normal CCDF and log-normal CCDF exhibited comparable performance, especially the latter had the highest R^2. By contrast, as shown in Fig. 15, SK 5, one of the profiles in South Kaiapoi that generally behaved as the block-mode failure featuring a double-curvature displacement distribution, normal CCDF and log-normal CCDF gave more sucessful approximation, especially the former had a R^2 approaching 0.9, whereas the exponential decay had the lowest R^2 of below 0.5.

The estimated parameters of all the profiles in Kaiapoi are summarized in Table 3, and the values of R^2 are compared in Fig. 16. In North Kaiapoi, as shown in Fig. 16(a), the logarithmic decay and log-normal CCDF showed consistently good performance (above 0.8 except for NK1), and normal CCDF and exponential decay can also be considered satisfactory for profiles other than NK1. However, for NK1 that can be categorized as block-mode failure, the exponential decay failed to approximate the ground displacement. On the other hand, for profiles in South Kaiapoi, the normal CCDF and log-normal CCDF generally gave better approximation of the double-curvature distribution than the others, whereas the exponential decay was considered the worst because its R^2 lower than 0.5 in a majority of the profiles.

4.4 Dominant Factors of Surface Displacement Distribution

As presented in the previous sections, a majority of the surface displacement curves show more significant decay near the waterfront, and thus the logarithmic decay model can be more generally applied to different cases for approximation. However, some curves showed a double-curvature feature, especially in South Kaiapoi, and are best fitted by the normal and log-normal CCDF. This feature was relevant to the "block-mode" failure, namely, the ground moved as blocks with large intermediate fissures. Therefore, the factors that may dominate the type of surface displacement distribution are discussed in this section.

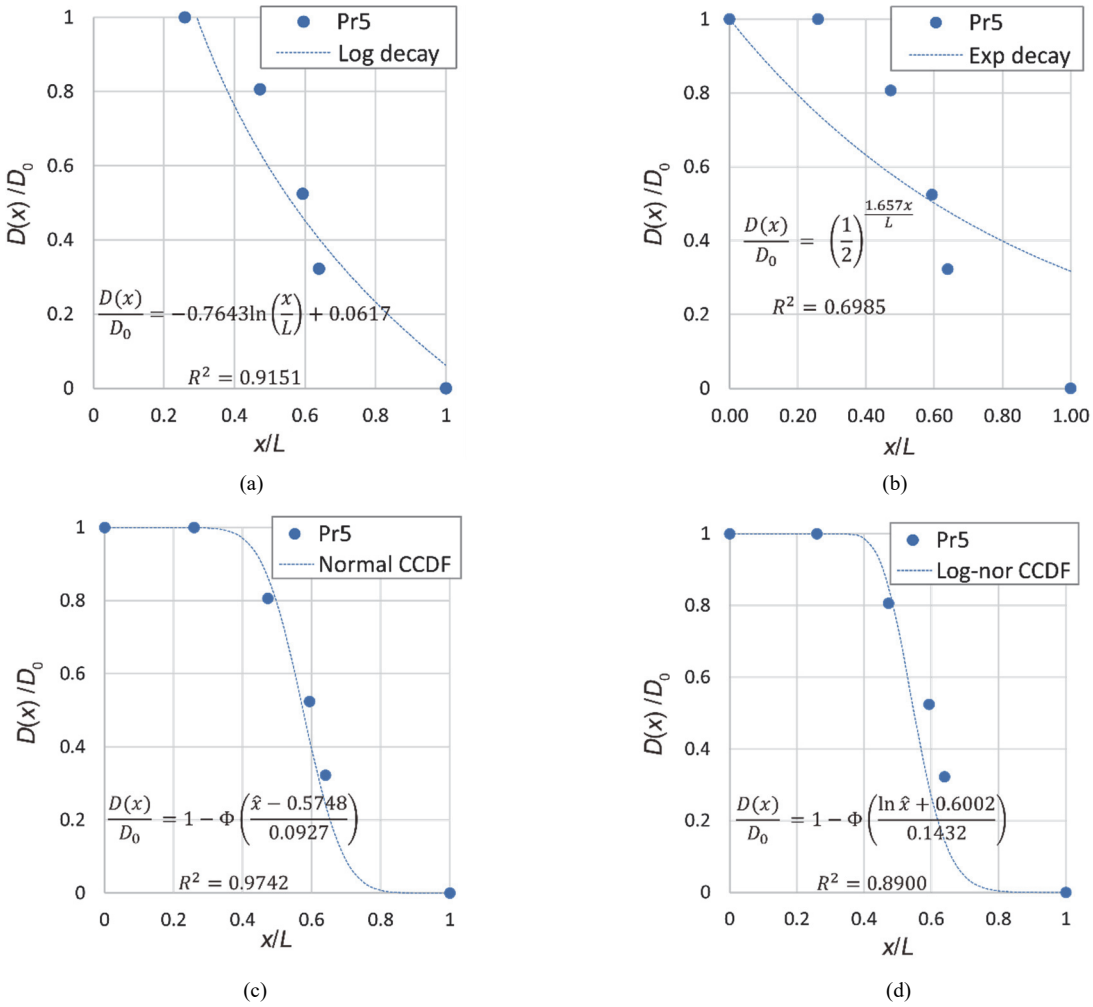

Fig. 12 Surface displacement regression of profile Pr5 in central Taiwan during 1999 Chi-Chi earthquake: (a) logarithmic decay; (b) exponential decay; (c) normal CCDF; (d) log-normal CCDF

Table 2 Estimated model parameters of surface displacement regression in central Taiwan during 1999 Chi-Chi earthquake

Profile	Logarithmic decay			Exponential decay	
	a	*b*	R^2	*c*	R^2
Pr1	– 0.4524	0.1406	0.8589	2.641	0.8331
Pr2	– 0.6511	– 0.0017	0.8627	3.142	0.7813
Pr3	– 0.4540	0.1004	0.9311	1.950	0.9610
Pr4	– 0.4570	0.0189	0.9630	3.102	0.9046
Pr5	– 0.7643	0.0617	0.9151	1.657	0.6985
Pr6	– 0.5080	– 0.0215	0.9983	3.320	0.8746
Profile	Normal CCDF			Log-normal CCDF		
	$\hat{\mu}$	$\hat{\sigma}$	R^2	$\hat{\mu}^*$	$\hat{\sigma}^*$	R^2
Pr1	0.6287	0.1092	0.8795	– 0.6286	0.2286	0.8440
Pr2	0.5974	0.0962	0.5596	– 0.5806	0.1456	0.5340
Pr3	0.4455	0.0972	0.9219	– 1.046	0.2445	0.7720
Pr4	0.4719	0.0960	0.7550	– 0.9515	0.2255	0.6572
Pr5	0.5748	0.0927	0.9742	– 0.6002	0.1432	0.8900
Pr6	0.4994	0.0953	0.8159	– 0.8642	0.2135	0.9479

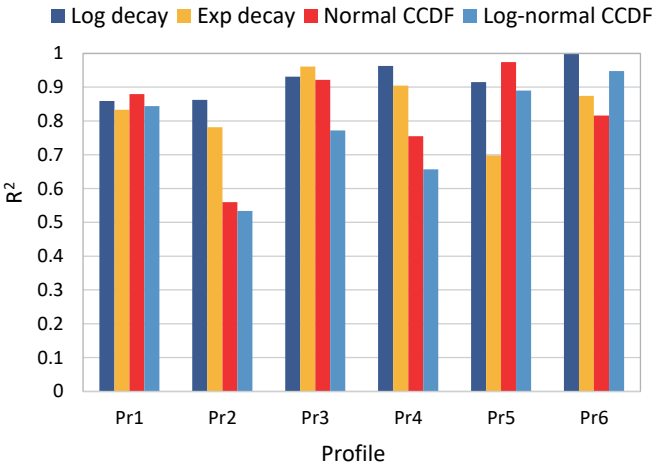

Fig. 13 Comparison of R-squared values of surface displacement regression in central Taiwan during 1999 Chi-Chi earthquake

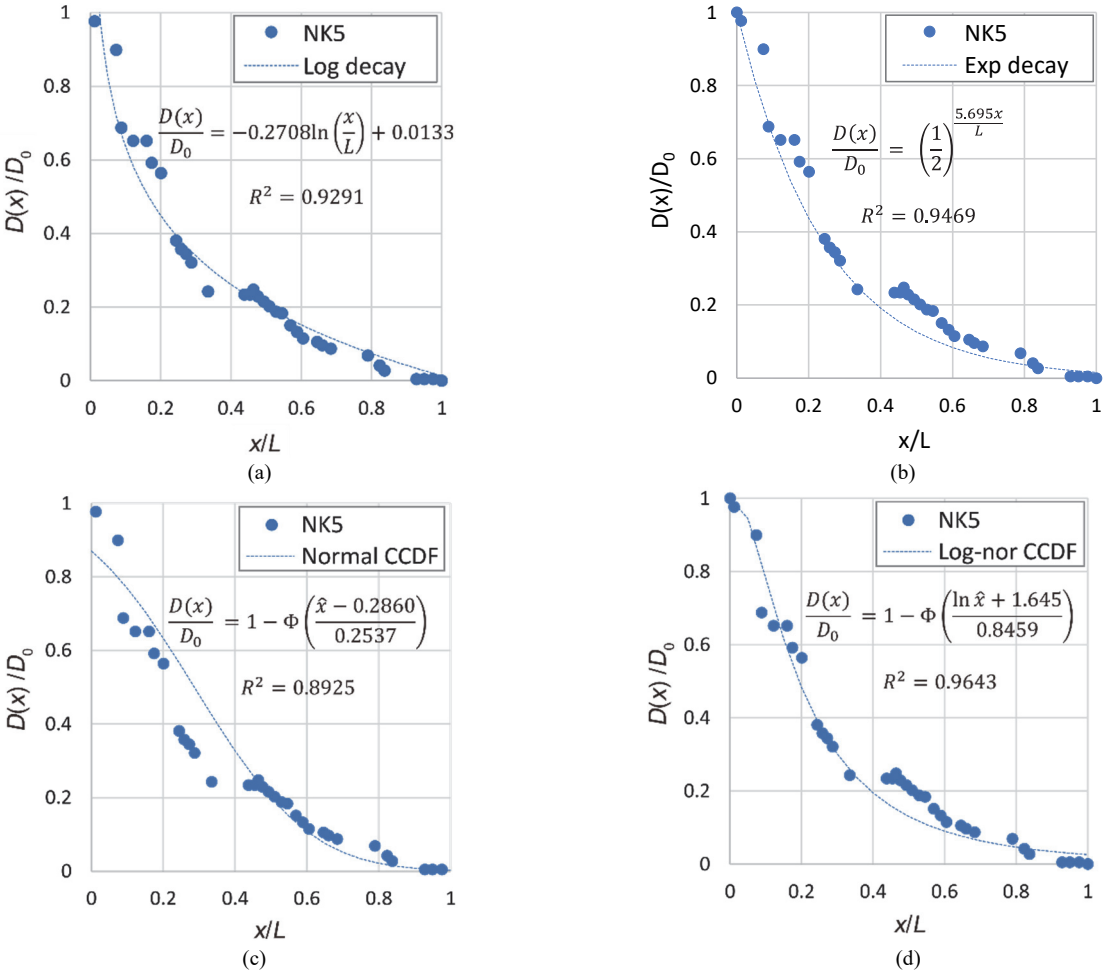

Fig. 14 Surface displacement regression of profile NK5 in south Kaiapoi during 2010 Darfield earthquake: (a) logarithmic decay; (b) exponential decay; (c) normal CCDF; (d) log-normal CCDF

Site conditions such as the soil profile, the groundwater table, and the slope angle, as well as the characteristics of ground motion, are relevant to liquefaction-induced lateral spreading. The sites investigated in this study are all waterfront sites that generally have a gentle slope and a high groundwater table so that these two are probably not the dominant factors. On the other hand, the soil profiles and ground motions are different from case to case and could be influential. Despite the common long-period feature of the ground motions in all three cases, that in Kaiapoi during the 2010 Darfield earthquake had an extremely long period. In addition, the lateral spreading in South Kaiapoi occurred on paleochannel with very soft and loose soil. Therefore, the "block-mode" failure in South Kaiapoi might be attributed to the combination of very long-period ground motion and very weak deposit.

It is further noted that, as mentioned in Section 3.2, towards-free-face lateral spreading occurred at wharves with massive caisson quay wall showed different surface displacement distribution from that at riverbanks possibly because of the inertial effect of retaining structures.

Because of limited data, what above are only preliminary discussions, and further study in the future is necessary for identification and evaluation of all important factors that dominate surface displacement distribution of lateral spreading as well as deduction of corresponding mechanisms.

5. LENGTH OF TOWARDS-FREE-FACE LATERALLY SPREADING AREA

To examine the relationship the surface displacement at waterfront (D_0) and the length of laterally spreading area (L), the L versus D_0 plot in each investigated case are given in Figs. 17 to 19 with the lines representing the mean and mean plus/minus one standard deviation (denoted as μ, $\mu + \sigma$, and $\mu - \sigma$) of L/D_0 ratio marked to highlight the range with a probability of 68% assuming L/D_0 values are in normal distribution. Note that because only the data of three earthquake events at limited sites are included, the results only represent the characteristics of each case rather than a general trend.

For the lateral spreading in the Port of Kobe during 1995 Hanshin Awaji earthquake, L/D_0 values of survey lines with north and south facing quay walls were merged to calculate μ and σ for their similar tendency. Figure 17 shows that the 68% probability range of L/D_0 is about 18-80 with a mean of approaching 50, which is not surprisingly close to the suggestion of Tokimatsu and Asaka (1998), L/D_0 ranged 25-100 with a representative of 50, because of the data from the same site. The central Taiwan case of 1999 Chi-Chi earthquake had a L/D_0 range of 11-86 corresponding to a probability of 68% with a mean of close to 50, as shown in Fig. 18, which is not far from the previous case. For the lateral spreading

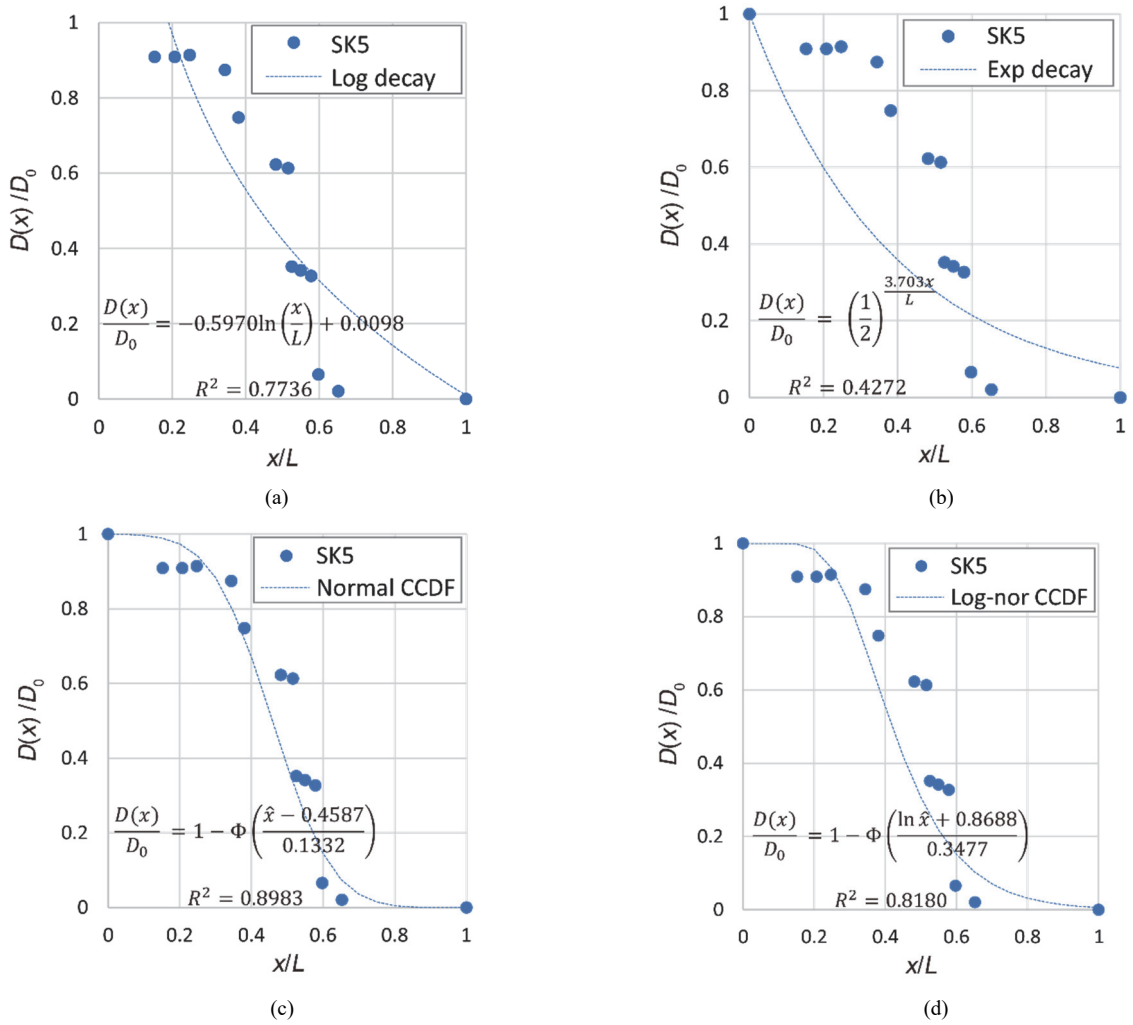

Fig. 15 Surface displacement regression of profile SK5 in North Kaiapoi during 2010 Darfield earthquake: (a) logarithmic decay; (b) exponential decay; (c) normal CCDF; (d) log-normal CCDF

Table 3 Estimated model parameters of surface displacement regression in Kaiapoi during 2010 Darfield earthquake: (a) North Kaiapoi; (b) South Kaiapoi

(a)

Profile	Logarithmic decay			Exponential decay	
	a	*b*	R^2	*c*	R^2
NK1	– 0.6042	0.2918	0.6186	2.515	0.0748
NK 3	– 0.2157	0.0306	0.8628	4.206	0.7753
NK 4	– 0.4306	– 0.0868	0.9062	5.689	0.7685
NK 5	– 0.2708	0.0133	0.9291	5.965	0. 9469
NK 6	– 0.4207	– 0.0627	0.8888	6.196	0.8257
NK 8	– 0.4752	– 0.0159	0.9476	3.427	0.9663
NK 9	– 0.2468	– 0.1111	0.8151	8.503	0.8742
Profile	Normal CCDF			Log-normal CCDF		
	$\hat{\mu}$	$\hat{\sigma}$	R^2	$\hat{\mu}^*$	$\hat{\sigma}^*$	R^2
NK1	0.6930	0.1518	0.6112	– 0.3891	0.3169	0.6100
NK 3	0.1278	0.4751	0.7129	– 2.028	1.316	0.9115
NK 4	0.3022	0.1529	0.9057	– 1.368	0.5693	0.8812
NK 5	0.2860	0.2537	0.8925	– 1.645	0.8459	0.9643
NK 6	0.3814	0.2107	0.7637	– 1.352	0.5630	0.9167
NK 8	0.3736	0.2333	0.8524	– 0.9749	0.5094	0.9909
NK 9	0.1236	0.2371	0.7145	– 2.401	0.9065	0.9418

(b)

Profile	Logarithmic decay			Exponential decay	
	a	*b*	R^2	*c*	R^2
SK5	– 0.5970	0.0098	0.7736	3.703	0.4272
SK6	– 0.4018	0.4166	0.3419	1.556	0.3762
SK7	– 0.3307	0.3136	0.4892	2.185	0.5357
SK8	– 0.3026	0.2743	0.4436	2.822	0.3843
SK9	– 2.2462	– 0.2794	0.6924	2.632	0.0406
SK10	– 0.7999	– 0.0742	0.7919	4.083	0.5499
SK11	– 0.3596	0.1994	0.7253	3.180	0.6388
Profile	Normal CCDF			Log-normal CCDF		
	$\hat{\mu}$	$\hat{\sigma}$	R^2	$\hat{\mu}^*$	$\hat{\sigma}^*$	R^2
SK5	0.4587	0.1332	0.8983	– 0.8688	0.3477	0.8176
SK6	0.8351	0.5182	0.7229	– 0.2455	0.2996	0.5838
SK7	0.7270	0.2073	0.8920	– 0.4577	0.5018	0.7269
SK8	0.6733	0.1436	0.5733	– 0.5659	0.3991	0.4458
SK9	0.6945	0.0404	0.8705	– 0.3701	0.0578	0.8649
SK10	0.5195	0.1870	0.8666	– 0.6709	0.2922	0.8881
SK11	0.4960	0.2605	0.8648	– 0.8578	0.6055	0.8587

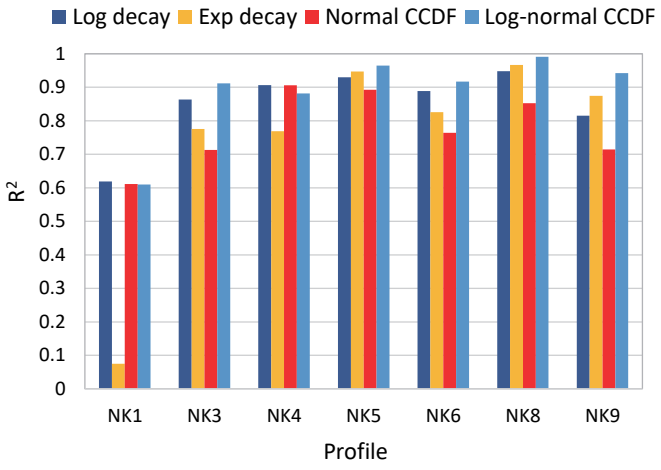

(a)

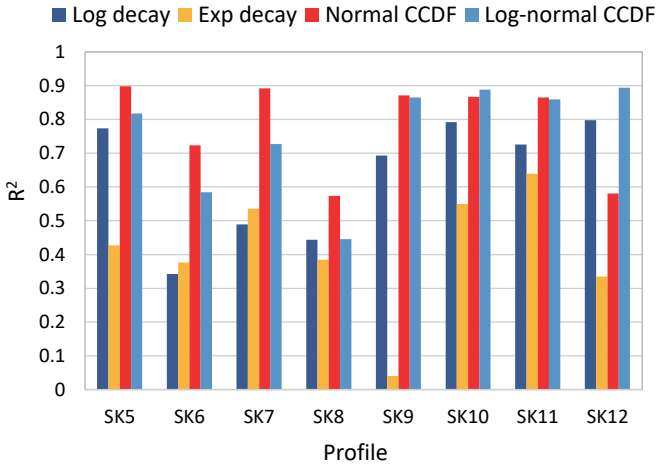

(b)

Fig. 16 Comparison of R-squared values of surface displacement regression in Kaiapoi during 2010 Darfield earthquake: (a) North Kaiapoi; (b) South Kaiapoi

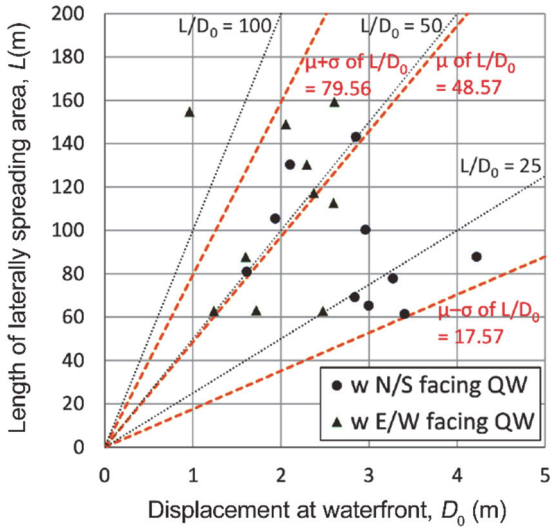

Fig. 17 *L* versus D_0 plot of lateral spreading in the Port of Kobe during 1995 Hanshin Awaji earthquake

in Kaiapoi during 2010 Darfield earthquake, because the D_0 values at profiles NK1 and NK3 were lower than 0.5 m, leading to extremely large L/D_0 values (over 400), their data were excluded so as not to distort the calculation of μ and σ. In addition, since the L/D_0 values of North and South Kaiapoi showed certain discrepancy possibly because their displacement distribution showed different tendency, the calculation of μ and σ was made separately. Figure 19 depicted that the L/D_0 ranges of both North and South Kaiapoi are larger than the other two cases; the 68% probability range of L/D_0 of the former is around 68-118 with a mean of about 93, whereas that of the latter is even larger, around 105-209 with a mean of about 157. These discrepancies are possibly due to the differences in the geographical, geological, and soil conditions of the sites, *e.g.,* the quite weak paleochannel deposit in South Kaiapoi has the largest L/D_0 value, and worthy of further investigation in the future.

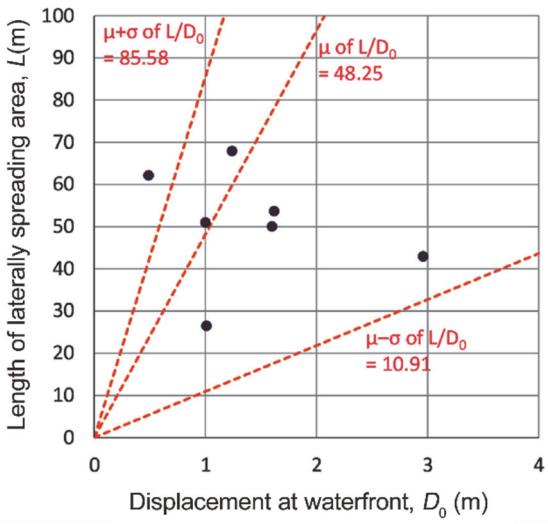

Fig. 18 *L* versus D_0 plot of lateral spreading in central Taiwan during 1999 Chi-Chi earthquake

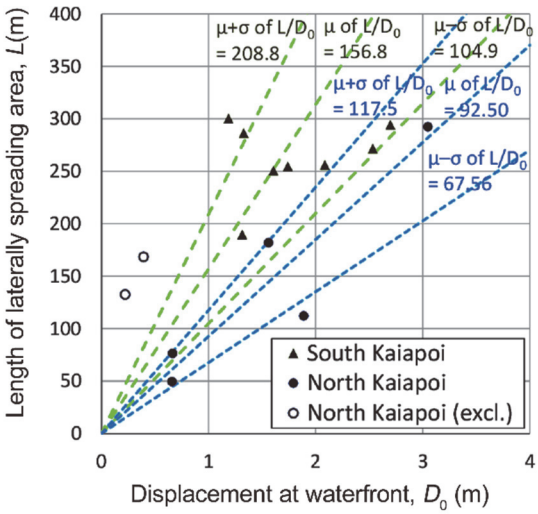

Fig. 19 *L* versus D_0 plot of lateral spreading in Kaiapoi during 2010 Darfield earthquake

6. CONCLUSIONS

According to selected field measurement data of surface displacement caused by lateral spreading of liquefied ground and corresponding regression analysis using different distribution models, the following conclusions can be drawn:

1. In the case of Port of Kobe during the 1995 Hanshin Awaji earthquake, the decay of displacement with the distance to the waterfront was most significant near the waterfront possibly because of the inertia effect of the caisson quay walls, and both the logarithmic decay and exponential decay models gave satisfactory approximation of the displacement distribution.
2. As for the central Taiwan case during the 1999 Chi-Chi earthquake, the surface displacement attenuated not as significant as in the previous case. The logarithmic decay exhibited consistently good performance in all the profiles, whereas normal and log-normal CCDF successfully approximated the displacement distribution of profiles with a double-curvature feature.
3. Regarding the 2010 Darfield earthquake, surface displacement of most examined profiles in North Kaiapoi exhibited similar distribution as the Port of Kobe case, and the regression by all the models can be considered satisfactory. By contrast, block-mode failure was generally caused in South Kaiapoi, possibly owing to the combination of extremely long-period ground motion and quite weak deposit, and the normal and log-normal CCDF gave good approximation of the surface displacement for its double-curvature feature.
4. To sum up, the logarithmic decay model is most widely applicable for approximating the surface displacement of laterally spreading ground, and the exponential decay model is appropriate for that showing most significant decay near the waterfront; whereas normal and log-normal CCDF show good performance for the block-mode failure that features a double-curvature distribution.
5. Based on the statistics of L/D_0 ratio from field data of Port of Kobe and central Taiwan, L/D_0 generally ranged from 10 to 85 and a representative of 50 can be specified, which is roughly conformable to Tokimatsu and Asaka (1998). However, in the Kaiapoi case the L/D_0 ratio was much larger and further investigation may be needed.
6. In this study, the regression coefficients of adopted models are different for each site and each survey line because the geographical, geological, and soil conditions are influential but are not separately considered. Hence, the results only revealed qualitative tendencies but cannot be used for quantitative prediction. In the future the influence of these factors should be further investigated and clarified, and thus the prediction models for different distribution types, such as the MLR procedure for logarithmic decay (Youd *et al.* 2002), can be proposed.

FUNDING

This study was financially supported by the Ministry of Science and Technology, Taiwan (Research Project MOST 110-2221-E-006-048-MY3).

DATA AVAILABILITY

The raw data used in this study are available from the cited works, and the data generated in this study are included in this paper.

CONFLICT OF INTEREST STATEMENT

The authors declare that there is no conflict of interest.

REFERENCES

Cubrinovski, M. and Robinson, K. (2016). "Lateral spreading: Evidence and interpretation from the 2010–2011 Christchurch earthquakes." *Soil Dynamics and Earthquake Engineering*, **91**, 187-201. https://doi.org/10.1016/j.soildyn.2016.09.045

Bradley, B. A. (2012). *Ground Motion and Seismicity Aspects of the 4 September 2010 Darfield and 22 February 2011 Christchurch Earthquakes*, Technical Report Prepared for the Canterbury Earthquakes Royal Commission, Christchurch, New Zealand.

Cubrinovski, M., Robinson, K., Taylor, M., Hughes, M., and Orense, R. (2012). "Lateral spreading and its impacts in urban areas in the 2010–2011 Christchurch earthquakes." *New Zealand Journal of Geology and Geophysics*, **55**(3), 255-269. https://doi.org/10.1080/00288306.2012.699895

FEMA (Federal Emergency Management Agency) (1999). *Earthquake Loss Estimation Methodology HAZUS 99 Technical Manual*. Federal Emergency Management Agency / National Institute of Building Sciences, Washington, D.C.

Hamada, M. (1992). "Large ground deformations and their effects on lifelines: 1964 Niigata Earthquake." In: Hamada, M. and O'Rourke T.D (Eds.) *Case Studies of Liquefaction and Lifeline Performance during Past Earthquakes*, 1 – Japanese Case Studies, Technical Report NCEER-92-0001, 3-1–3-123.

Hwang, J. H., Yang, C. W., Tan, C. H., and Chen, C. H. (2000). "Investigation on soil liquefactions during the Chi-Chi earthquake." *Sino Geotechnics*, **77**, 51-64 (in Chinese).

Iai, S., Sugano, T., Morita, T., and Ichii, K. (1997). "Seismic performance of quay walls -Kobe Earthquake-." *Proceedings of Earthquake Criteria Workshop*, Yokohama, Japan, 1-29.

Ishihara, K., Yoshida, K., and Kato, M. (1997). "Characteristics of lateral spreading in liquefied deposits during the 1995 Hanshin-Awaji earthquake." *Journal of Earthquake Engineering*, **1**(1), 23-55. https://doi.org/10.1080/13632469708962360

Iwasaki, Y. and Tai M. (1996). "Strong motion records at Kobe Port Island." *Soils and Foundations*, **36**(SP), 29-40. https://doi.org/10.3208/sandf.36.Special_29

Lin, C. C. (2002). *Lateral Spreading in Wufeng Area during 1999 Chi-Chi Earthquake*, Master Thesis, National Chung Hsing University, Taiching, Taiwan (in Chinese).

Lin, S. S., Tseng, Y. J., Liao, J. C., Wang, C. H., and Lee, W. F. (2006). "Ground lateral spread effects on single pile using uncoupled analysis method." *Journal of GeoEngineering*, **1**(2), 51-62. https://doi.org/10.6310/jog.2006.1(2).1

Madabhushi, S. P. G. (1995). *Strong Motion at Port Island during the Kobe Earthquake*, Cambridge University Publication CUED/D-SOILS/TR285, Cambridge, UK.

Pavlenko, O. V. and Wen, K. L. (2008). "Estimation of nonlinear soil behavior during the 1999 Chi-Chi, Taiwan, earthquake."

Pure and Applied Geophysics, **165**, 373-407. https://doi.org/10.1007/s00024-008-0309-9

Rauch, A. F. (1997). *EPOLLS: An Empirical Method for Predicting Surface Displacements Due to Liquefaction– Induced Lateral Spreading in Earthquakes*, Ph.D. Dissertation, Virginia Polytechnic Institute and State University, VA.

Robinson, K. M. (2016). *Liquefaction-Induced Lateral Spreading in the 2010–2011 Canterbury Earthquakes*, PhD Dissertation, University of Canterbury.

Shamoto, Y. and Hotta, H. (1996). "Measurement of lateral ground displacement in Rokko Island." *Proceedings of 31st Japan National Conference on Geotechnical Engineering*, Tokyo, Japan, **1**, 1251-1252 (in Japanese).

Tokimatsu, K. and Asaka, Y. (1998). "Effects of liquefaction-induced ground displacements on pile performance in the 1995 Hyogoken-Nambu earthquake." *Soils and Foundations*, **38**(Special), 163-177. https://doi.org/10.3208/sandf.38.Special_163

Tokimatsu, K., Oh-Oka, H., Shamoto, Y., Nakazawa, A., and Asaka, Y. (1997). "Failure and deformation modes of piles caused by liquefaction-induced lateral spreading in the 1995 Hyogoken-Nambu earthquake." *Proceedings of 3rd Kansai International Forum on Comparative Geotechnical Engineering*, Kobe, Japan, 239-248.

Yasuda, S., Ishihara, K., Harada, K., and Nomura, H. (1997). "Area of ground flow occurred behind quay walls due to liquefaction." *Proceedings of 3rd Kansai International Forum on Comparative Geotechnical Engineering*, Kobe, Japan, 85-93.

Youd, T. L. (2018). "Application of MLR procedure for prediction of liquefaction-induced lateral spread displacement." *Journal of Geotechnical and Geoenvironmental Engineering*, ASCE, **144**(6), 04018033. https://doi.org/10.1061/(ASCE)GT.1943-5606.0001860

Youd, T. L. (2014). "Ground failure investigations following the 1964 Alaska earthquake." *Proceedings of 10th U.S. National Conference on Earthquake Engineering Frontiers of Earthquake Engineering (10NCEE)*, Anchorage, AK.

Youd, T. L. (1995). "Liquefaction-induced lateral ground displacement." *Proceedings of 3rd International Conference on Recent Advances in Geotechnical Earthquake Engineering and Soil Dynamics*, II, St. Louis, MS, 911-925.